

## **CHAPTER 2: BACKGROUND**

The extremely small size and outstanding physical properties of carbon nanotubes have interested researchers in a wide variety of fields, including chemistry, physics, materials science, and engineering. This interest is from both the standpoint of fundamental research into material behavior, as well as the use of carbon nanotubes in a variety of applications (as discussed in Chapter 1), where the characteristics of the nanotubes can be exploited to gain a design advantage. With the explosion of research in the area of nanotechnology, the potential application of nanotubes (and other nanostructures) is quite large, and several excellent books broadly discuss the early work in this field (Drexler 1992; Dresselhaus, Dresselhaus et al. 1996; Harris 1999).

In this dissertation we will primarily focus on the use of carbon nanotubes as the reinforcing phase in a bulk polymer material, with a focus on the effective mechanical response of the material to low levels of stress. While this narrow focus will neglect a wide variety of interesting topics, such as the electrical, thermal, and fracture behavior of nanotube-reinforced polymers, we believe that the results presented in this dissertation will provide a strong foundation for future characterization and development of NRP systems.

From the standpoint of modeling, nanotubes and their use in polymers are challenging because of the range of length scales that must be modeled for such materials. Modeling at atomistic scales using the principles of quantum mechanics and molecular dynamics has been developed to model clusters of atoms, but are computationally prohibitive and to date have been limited to looking at the behavior of individual nanotubes. For larger length scales, the fields of micromechanics and continuum mechanics are well established but not well-suited to model details at the atomistic level that are likely to be important for nanostructured materials. The area of nanomechanics is proposed as a means to bridge these length scales in order to develop accurate models of nanotubes and related materials. The development of nanomechanics into a well-grounded area of study will require contributions from these other length scales as shown in Figure 1. Additional information provided by experimental techniques, at both the micro- and nano-scale, will further the development of these models.

The work described in this dissertation is an initial thrust in this direction; these efforts can be characterized as extending traditional micromechanics and viscoelastic models for the study of nanotube-reinforced polymers. This work is motivated by theoretical predictions and preliminary experimental results that suggest that small amounts of carbon nanotubes can significantly enhance the overall mechanical behavior of the polymer (Schadler, Giannaris et al. 1998; Shaffer and

Windle 1999; Gong, Liu et al. 2000; Qian, Dickey et al. 2000; Andrews, Jacques et al. 2002). Other types of nanoscale inclusions, including boron nitride (BN) nanotubes (Bengu and Marks 2001; Demczyk, Cumings et al. 2001), graphite nanoplatelets, nanoclays, and nanowires, while not directly addressed here, have also been proposed as candidate filler materials. NRPs hold vast potential as structural materials due to the extremely high strength- and modulus-to-weight ratios that are likely to be achieved with such materials. Other potential advantages of NRPs include multifunctionality, increased energy absorbance, higher toughness, and ease of manufacturing (particularly if the NRPs can be processed using traditional polymer techniques). Despite the challenges which these materials present in terms of modeling, processing, and most notably the availability and cost of the raw nanotube material, the preliminary results and inherent potential suggest that further study of NRPs is warranted.

In the remainder of this chapter we will introduce the reader to pertinent topics regarding both carbon nanotubes and their use as a reinforcing phase in polymeric materials. This background information will serve as a foundation for later chapters, where we will present models and experimental methodology that have been developed to study the mechanical response of nanotube-reinforced polymers.

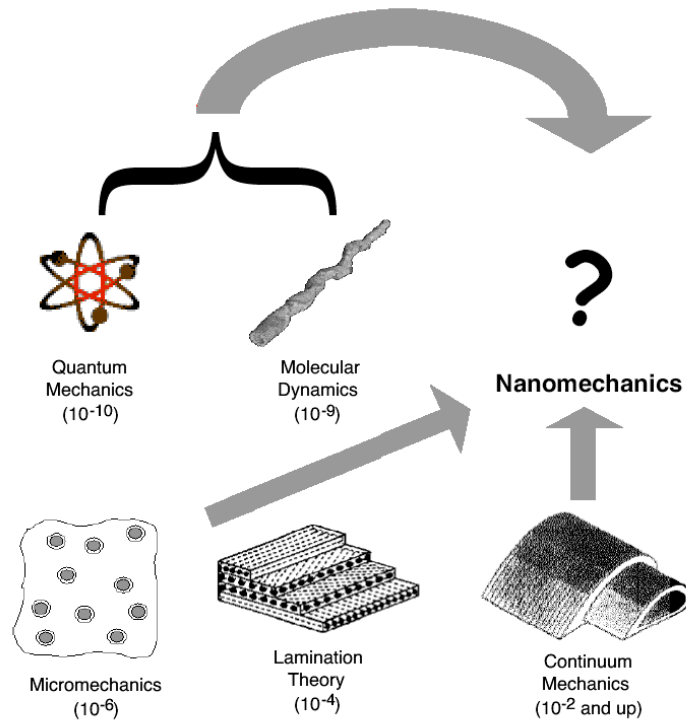


**Figure 1. Nanomechanics and other modeling length scales.**

## Structure of Carbon Nanotubes

Due to the inherent strength of the carbon-carbon bond and the potential of a defect-free structure, it has been suggested that nanotubes may approach the theoretical limits for many important mechanical properties, including axial stiffness and tensile strength. Large increases in fracture strain and toughness, and superior electrical/thermal properties, are other potential benefits of using NTs as the filler material in a polymer-based composite.

The outstanding properties that are predicted (and in some cases verified experimentally) for carbon nanotubes are the result of their structure, which can be pictured as being formed by rolling a graphene sheet into a cylinder. Because the graphene hexagonal lattice can be rolled at different angles, the geometry of a particular nanotube is best described in terms of the unit cell of the carbon nanotube, as shown in Figure 2. The atomic arrangement of the carbon nanotube is described by the chiral vector, which is defined by  $C_h = n\hat{a}_1 + m\hat{a}_2$ , where  $\hat{a}_1$  and  $\hat{a}_2$  are unit vectors on the hexagonal lattice and  $n$  and  $m$  are integers. Using this description the chiral angle ( $\theta$  in Figure 2) and diameter of the nanotube are given as

$$\theta = \tan^{-1} \left( \frac{3n}{2m+n} \right), \quad (1)$$

$$d_t = \frac{3}{\pi} a_{C-C} \sqrt{m^2 + mn + n^2}, \quad (2)$$

where  $a_{C-C}$  is the distance between neighboring carbon atoms in a flat graphene sheet (approximately 0.142 nm). As shown in Figure 3, nanotubes with different chiral vectors  $(n,m)$  will have different atomic configurations.

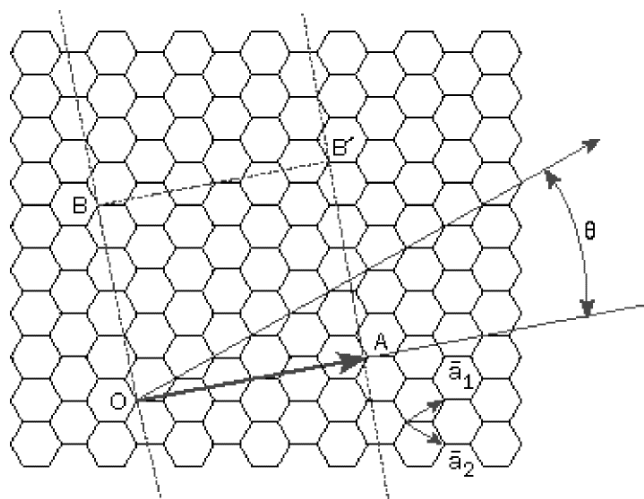


**Figure 2. Unit cell and chiral vector for a (4,2) carbon nanotube.**

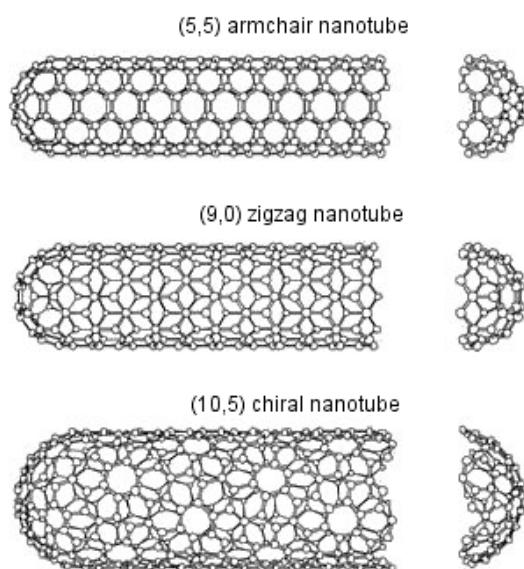


**Figure 3. Examples of nanotubes with different chirality.**

Certain nanotube properties have been found to be strongly dependent on the chirality of the nanotube, including electrical resistivity and fracture behavior. For example, a carbon nanotube will be metallic when the chiral vector satisfies the relationship  $n - m = 3q$ , where  $q$  is an integer, while all other nanotubes will be semiconductive. It has been estimated that 1/3 of all nanotubes are metallic. However, other properties, and in particular the stiffness, have been found to be relatively independent of the chirality. For our modeling work presented later in this dissertation we assume that chirality effects are negligible.

Carbon nanotubes can be further classified into three broad categories: single-walled nanotubes (SWNT), multi-walled nanotubes (MWNT), and nanotube bundles or ropes. SWNTs consist of a single layer of carbon atoms wrapped into a cylindrical shape, which may or may not be capped on each end by one half of a fullerene molecule (see Figure 3). Typical diameters for SWNTs are on the order of 1 nm, while lengths are often on the order of  $\mu\text{m}$ . This results in very large aspect ratios, which in traditional composites theory are desirable from the perspective of load transfer. Both the diameter and the length of the SWNTs are typically dependent on the particular technique used to create the nanotubes.

MWNTs consist of several concentric layers (or shells) of individual carbon nanotubes that are weakly coupled to each other through van der Waals forces. A high resolution transmission electron microscope (TEM) image of a MWNT is shown in

Figure 4 (Harris 1999). The spacing between these individual shells is on the order of 0.34 nm, which is slightly larger than the interlayer spacing in a graphene sheet. The diameter and number of shells comprising a MWNT is again dependent on the fabrication process, although diameters on the order of 30 nm may be considered as a ballpark estimate (Pan, Xie et al. 1999; Qian, Dickey et al. 2000).

Typically, nanotubes are found to have self-organized into crystalline bundles (Thess, Lee et al. 1996; López, Rubio et al. 2001), consisting of several to hundreds of SWNTs or MWNTs arranged in a closest-packed two-dimensional lattice. Within these bundles the nanotubes normally display a monodisperse range of diameters, with adjacent tubes weakly coupled via van der Waals interactions. A high resolution TEM image of a SWNT bundle is shown in Figure 5 (Journet, Maser et al. 1997), where the bundle is seen to consist of approximately 20 SWNTs of almost uniform diameter packed in a triangular lattice. The average tube diameter in the bundle is 1.4 nm, and the average spacing between the tubes was reported as 1.7 nm.

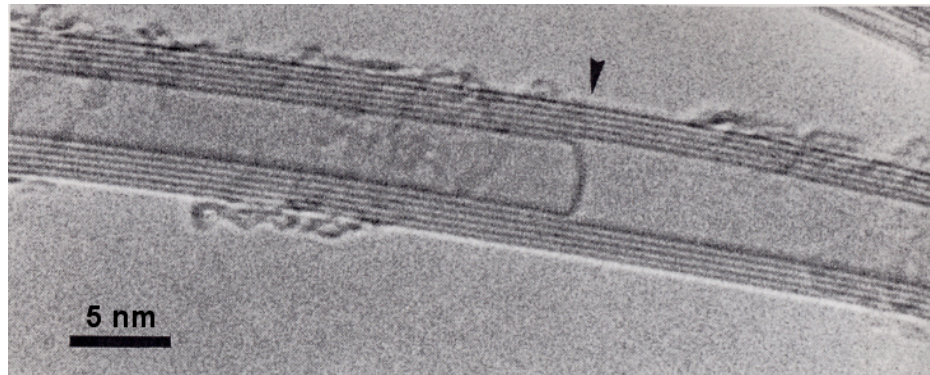


**Figure 4. High resolution TEM image of a MWNT with an internal cap highlighted by the arrow. (Harris 1999)**

While not modeled in the continuum approaches presented later in this work, explicit differences in the structural behavior of these various NT forms will need to ultimately be included in future models of nanotube-related materials. From the perspective of structural reinforcement, optimal behavior will be dependent on the proper transfer of load from the matrix to the inclusion (and among the shells or tubes in the case of MWNTs or NT bundles, respectively). While SWNTs are more susceptible to bending due to their extremely small cross-sections, for MWNTs and NT bundles interlayer sliding (so-called “sword and sheath” slippage (Yu, Yakobson et al. 2000)) and weak intertube coupling, respectively, could hinder load transfer between the phases. Such differences are not included in the models presented in this dissertation and will be the subject of future work.

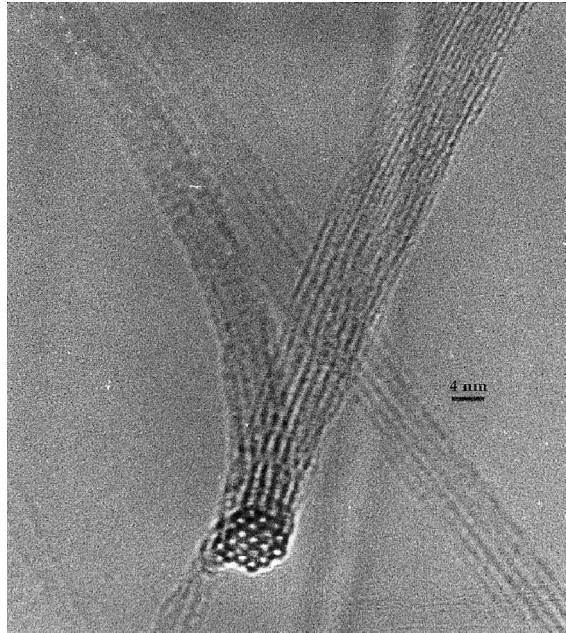


**Figure 5. High resolution TEM image of a SWNT bundle. (Journet, Maser et al. 1997)**

## **Methods of Nanotube Fabrication**

The properties of carbon nanotubes are closely related to their method of production. While an in-depth discussion of nanotube fabrication techniques is well beyond the scope of this dissertation, a summary of production techniques is included below for completeness. The reader is referred to the literature for a fuller description of work in this area.

A summary of some standard nanotube fabrication techniques is given in Table 1. A newer processing technique, flame synthesis, is also currently being developed

(Vander Wal and Tichich 2001). In early work the arc discharge and laser vaporizations processes were the most common forms of nanotube production, typically resulting in nanotubes with low structural defects and thus excellent physical properties. In these techniques SWNTs are typically formed in the presence of a metal catalyst, which seems to preclude the formation of MWNTs. One difficulty associated with these techniques is the need to process the end-product, which are typically found to be quite entangled (see Figure 6); in many cases amorphous carbon and other contaminants on the surface of the nanotubes need to be removed via various purifying techniques. An additional problem with these techniques is that production yields from these methods are rather limited, and do not seem suited to satisfy the long-term goal of ton-quantity production.

In the interest of developing a process that can be scaled for industrial production, a great deal of work has been devoted to techniques that may be classified as chemical vapor deposition (CVD) (Che, Lakshmi et al. 1998; Cassell, Raymakers et al. 1999). While CVD processes have been used to create a wide variety of carbon structures (Endo 1988), the major drawback of these methods is the reduced structural integrity of the nanotubes. For example, experimental work has suggested that the tensile moduli of CVD nanotubes may be more than an order of magnitude lower than those measured for nanotubes created via other methods (and hence with fewer structural defects) (Salvetat, Kulik et al. 1999). However, promising CVD techniques

that seem to produce nanotubes with fewer defects (and hence better physical properties) are currently under development (Cassell, Raymakers et al. 1999).

| <b>Method</b>   | <b>Arc discharge (carbon arc) (Ebbesen and Ajayan 1992)</b> | <b>Chemical vapor deposition (CVD) (Endo 1988)</b> | <b>Laser ablation (vaporization) (Thess, Lee et al. 1996)</b> | <b>High-pressure CO conversion (HiPCO) (Bronikowski, Willis et al. 2001)</b> |
|-----------------|---|--|---|--|
| <b>Summary</b>  | Graphite evaporated by a plasma via high currents           | Decomposition of a carbon-based gas                | Graphite blasted with intense laser pulses                    | Metal catalysts nucleate SWNTs at high pressure and temperature              |
| <b>Yield</b>    | 30%   | 20 to ~100 %                                       | Up to 70%   | 95% purity, 10 g/day   |
| <b>Strength</b> | SWNT and MWNTs with few structural defects                  | Easiest to scale to industrial production          | Produces SWNTs; diameter control via reaction temperature     | Excellent structural integrity for a CVD process                             |
| <b>Weakness</b> | Tubes tend to be short and highly entangled                 | Typically MWNTs with a high density of defects     | More expensive than the other methods                         | Production rates still relatively low  |

**Table 1. Common methods of carbon nanotube production.**

One of the benefits of the CVD method is that the growth and alignment of the nanotubes can be controlled by the patterning of the catalyst (typically metal) particles, such that very regular nanotube arrays as shown in Figure 7 can be formed. Here the nanotubes are seen to align perpendicular to the surface on which the catalyst has been deposited; results suggest that the nanotubes can be patterned on any suitable

substrate (independent of the geometry) given sufficient conditions (Bower, Zhou et al. 2000). Using techniques such as these it may be possible to create nanotube-reinforced polymers where the arrangement of the nanotubes is ordered and well-controlled. Such control of the orientation, alignment, and dispersion of nanotubes *within* a polymer matrix will be necessary to optimize the material performance of these systems.

A great deal of recent research has focused on limiting the defects within the nanotubes (which are particularly detrimental from a mechanical property perspective), and increasing the production yields from nanotube processing techniques. At the moment this work is quite challenging because detailed models of nanotube growth are not well developed. However, as interest from scientific community continues to expand it is expected that nanotube fabrication techniques will continue to develop. While at the moment the rather limited availability and large expense of nanotubes are hindrances to research in this area, future advances are likely to relax these restrictions.

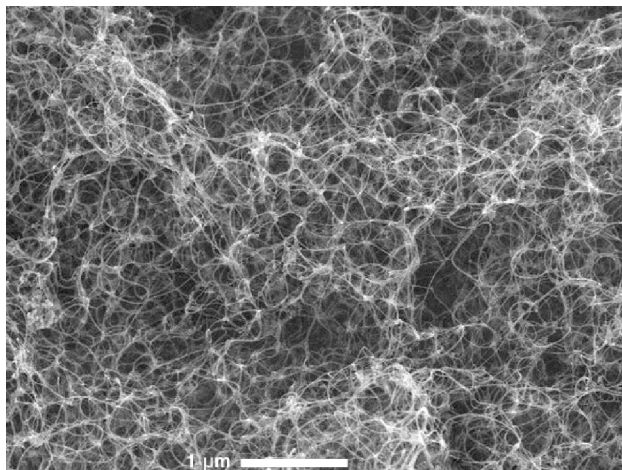


**Figure 6. SEM image of SWNT bundles formed via the arc discharge method.  
(Journet, Maser et al. 1997)**

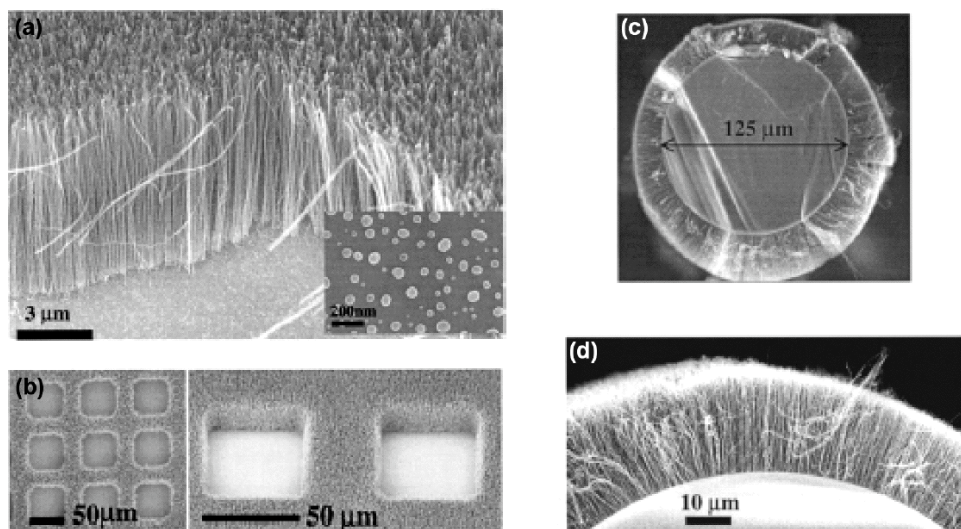


**Figure 7. SEM images of aligned MWNTs grown via microwave plasma enhanced chemical vapor deposition. (Bower, Zhou et al. 2000)**

## **Mechanical Properties of Carbon Nanotubes**

Because we are interested in the use of carbon nanotubes as a reinforcing phase within a polymer material, we will primarily focus on the mechanical properties of carbon nanotubes, a topic of intense research over the last few years. In this section we will review the initial theoretical and computation work in this area. We will also present recent experimental evidence that, despite the obvious complications associated with manipulating objects of such small size, has nonetheless tended to validate these predictions.

### ***Modulus***

Much of the initial work studying the mechanical properties of nanotubes has consisted of computational methods such as molecular dynamics and *ab initio* models. These models are primarily used to study SWNTs because of the increase in computational resources necessary to model systems comprised of a larger number of atoms. Typically these computational studies have found nominal values for the axial Young's modulus on the order of 1000 GPa (assuming a shell thickness of 0.34 nm), with values for the Poisson ratio approximately 0.20 to 0.30 (Gao, Çagin et al. 1998; Hernández, Goze et al. 1998; Che, Çagin et al. 1999; Sánchez-Portal, Artacho et al. 1999). Using an empirical force-constant method, elastic moduli of approximately 1

TPa were calculated for SWNTs and MWNTs, while values for SWNT bundles were between 0.4 and 0.8 TPa and found to be very dependent on the diameter of the individual tubes (Lu 1997). *Ab initio* calculations have found that the mechanical properties of nanotubes are similar to those of graphite down to small nanotube radii (on the order of 3 nm), at which point the properties increase due to the enhanced curvature of the tubes (Sánchez-Portal, Artacho et al. 1999)<sup>1</sup>. Most of these models assume defect-free nanotubes; nanotubes with a significant number of defects (such as those produced via CVD methods) are expected to have much lower moduli values (Salvetat, Kulik et al. 1999; Xie, Li et al. 2000).

More recently, a great deal of progress has been realized in the manipulating and testing of individual nanotubes and nanotube bundles (Treacy, Ebbesen et al. 1996; Falvo, Clary et al. 1997; Krishnan, Dujardin et al. 1998; Salvétat, Bonard et al. 1999; Salvétat, Briggs et al. 1999; Li, Cheng et al. 2000; Yu, Files et al. 2000; Yu, Kowalewski et al. 2000; Yu, Lourie et al. 2000). In general, the experimental results have validated the computational predictions. A summary of these experimental results is given in Table 2 (the reader is referred to the original sources for a more complete description of these methods). While a method of producing large quantities

---

<sup>1</sup> It should be noted that other researchers have suggested that, in order to properly model the bending behavior of the nanotubes, more appropriate values for the Young's modulus and the shell thickness would be on the order of 5 TPa and 0.067 nm, respectively (Yakobson, Campbell et al. 1997; Xin, Jianjun et al. 2000).

of nanotubes with uniform geometric and physical properties has yet to be developed, the high modulus of carbon nanotubes makes them an attractive candidate filler for composite materials.

### ***Strength***

Because strength is closely related to the presence of defects within a material, it has been hypothesized that nanotubes (particularly low defect NTs formed via carbon arc and laser vaporization methods) may approach theoretical limits in terms of strength. In a recent molecular mechanics simulation, NT fracture strains between 10 and 15% were reported, with corresponding tensile stresses on the order of 65 to 93 GPa (compare to the values for other common filler materials listed in Table 3) (Belytschko, Xiao et al. 2002).

| Type of NT  | Method  | Modulus Values   | Comments  |
|---|---|--|---|
| Laser ablated SWNTs<br>(Krishnan, Dujardin et al. 1998)                                 | Amplitude of thermal vibration within a TEM             | 1.3 -0.4/+0.6 TPa  | Weighted average value of 1.25 TPa                            |
| Laser ablated SWNT bundles<br>(Yu, Files et al. 2000)                                   | Nanostressing stage within a SEM                        | 320 to 1470 GPa, mean of 1002 GPa  | Load carried by SWNTs on rope perimeter                       |
| Carbon arc SWNT bundles<br>(bundle diameters 3-20 nm)<br>(Salvetat, Briggs et al. 1999) | Beam-bending via AFM                                    | ~ 1 TPa for 3 nm diameter, decreasing to < 0.1 GPa for larger diameter     | Estimated shear moduli of SWNT bundle on the order of 1 GPa   |
| Carbon arc MWNTs<br>(Poncharal, Wang et al. 1999)                                       | Electromechanical deflection and resonance within a TEM | ~ 1 TPa for small diameter (<10 nm) to 0.1 TPa for large diameter (>30 nm) | Modulus a strong function of diameter                         |
| Carbon arc MWNTs (Yu, Lourie et al. 2000)   | Nanostressing stage within a SEM                        | Modulus of outer shell from ~270 to ~950 GPa                               | Failure via "sword-in-sheath" mechanism                       |
| CVD and carbon arc MWNTs (Salvetat, Kulik et al. 1999)                                  | Beam-bending via AFM                                    | CVD: ~ 10-50 GPa<br>Arc: 810 -160/+410 GPa                                 | Order of magnitude increase after annealing CVD NTs at 2500°C |
| CVD MWNTs (Pan, Xie et al. 1999; Xie, Li et al. 2000)                                   | Miniature stress-strain tests on 2 mm NT ropes          | Young's modulus ~ 0.45 TPa<br>Tensile strength ~ 1.5-3.6 GPa               | Lower values attributed to defects in CVD tubes               |

**Table 2. Experimental values for the Young's modulus of carbon nanotubes.**

Novel experimental work looking at the fracture behavior of nanotubes has recently been carried out using a nanostressing stage located within an SEM (see Figure 8). For SWNT bundles the maximum tensile strain was estimated to be 5.3%, with the tensile strength of the individual SWNTs estimated to be 13 to 52 GPa (Yu, Files et al. 2000). Related tests on MWNTs found that failure occurred via a “sword-in-sheath” mechanism at tensile strains up to 12%, with the tensile strength of the outer shell of the MWNT estimated to be between 11 and 63 GPa (Yu, Lourie et al. 2000). The tensile strength of NTs has been estimated to be 3.6 GPa for CVD-grown MWNTs using a miniature stress-strain puller to test long (2mm) NT ropes, with the order of magnitude decrease in strength attributed to an increase in defects (Pan, Xie et al. 1999; Xie, Li et al. 2000).

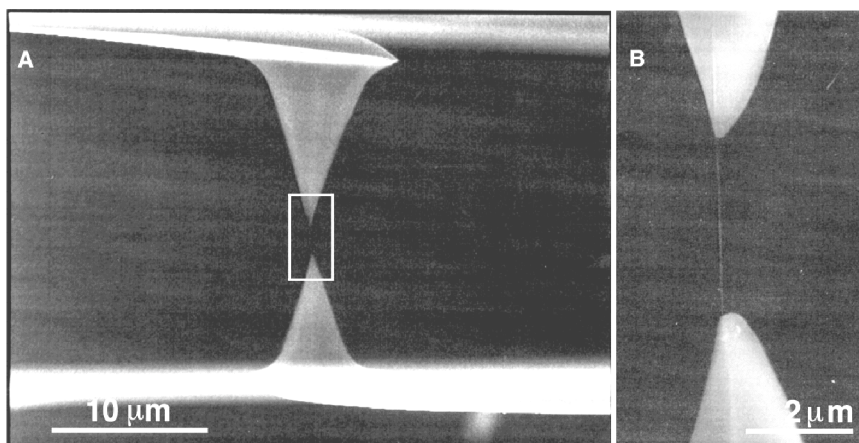


**Figure 8. SEM image of a MWNT loaded in tension between two AFM tips in a nanostressing stage. (Yu, Lourie et al. 2000)**

To place the nanotube moduli and strength predictions into proper perspective, representative values for common types of filler materials for structural reinforcement are given in Table 3. While the predicted properties of carbon nanotubes compare quite favorably to those materials listed in this table, a greater understanding of the nanotubes themselves, and issues related to their use within a polymer matrix, must be developed in order to fully utilize the properties of the nanotubes in structural composites. These issues will be discussed in the next section.

| <b>Fiber</b> | <b>Diameter (<math>\mu\text{m}</math>)</b> | <b>Density (<math>\text{g}/\text{cm}^3</math>)</b> | <b>Tensile strength (GPa)</b> | <b>Modulus (GPa)</b> |
|--------------|--|--|-------------------------------|----------------------|
| Carbon       | 7  | 1.66   | 2.4-3.1                       | 120-170              |
| S-glass      | 7  | 2.50   | 3.4-4.6                       | 90                   |
| Aramid       | 12   | 1.44   | 2.8                           | 70-170               |
| Boron        | 100-140                                    | 2.50   | 3.5                           | 400                  |
| Quartz       | 9  | 2.2  | 3.4                           | 70                   |
| SiC fibers   | 10-20                                      | 2.3  | 2.8                           | 190                  |
| SiC whiskers | 0.002                                      | 2.3  | 6.9                           | -                    |
| Carbon NTs   | 0.001-0.1                                  | $\sim 1.33$  | Up to $\sim 50$               | Up to $\sim 1000$    |

**Table 3. Filler materials for structural reinforcement. (Matienzo, Wang et al. 1994)**

## **Carbon Nanotube-Reinforced Polymers**

Given the moduli and strength values that have been predicted (and measured) for carbon nanotubes, they are potentially an ideal filler material for high performance (polymer) composite materials with outstanding modulus-to-weight and strength-to-weight ratios. However, to fully and efficiently utilize the exceptional properties of carbon nanotubes in NRPs for structural reinforcement, several issues related to the fabrication of the NRPs will need to be addressed. These issues are discussed in detail below. We will then present a review of some initial experimental results on NRPs that show promising mechanical property enhancements with the addition of relatively small amounts of carbon NTs. A summary of selected published work regarding carbon nanotube-reinforced polymers is given in the Appendix.

### ***Issues related to the fabrication of NRPs***

Although the fabrication of nanotube-reinforced polymers must be optimized in order to achieve ultimate effective properties, at the moment there are several critical issues that are not well understood in this area. While individual research groups have made significant processing advances for particular nanotube-polymer systems, universal guidelines regarding the fabrication of NRPs do not exist. This is in part due to the complexity of the polymer chemistry, the lack of detailed models

describing the processing conditions, and the large list of parameters (specific to the polymer and type of nanotube under consideration) that can influence the polymer-nanotube interaction and impact the effective NRP properties. Three of these issues are discussed in detail below.

### **Nanotube dispersion with the polymer**

One issue of practical importance for NRPs is the separation and dispersion of the nanotubes within the matrix, which is critical as the nanotubes tend to assemble into ropes or bundles due to van der Waals interactions between the individual tubes. While some researchers have been able to separate individual nanotubes from the bundles via ultrasound and polar solvents, maintaining separated nanotubes during the processing of NRPs is still the subject of ongoing work. Some results suggest that the use of a surfactant as a coupling agent may overcome van der Waals attractive force and allow good dispersion of the nanotubes within the polymer (Gong, Liu et al. 2000). However, it is unclear whether such processing agents can be employed to promote nanotube dispersion without compromising the nanotube-polymer interface.

### **Nanotube orientation**

Optimal material properties will only be achieved if the orientation of the nanotubes within the polymer can be controlled, and several techniques have been

proposed to address this issue. One group found that cutting thin slices (on the order of 100 nm) of a nanotube-reinforced epoxy film introduced preferential orientation via shear flow (Ajayan, Stephan et al. 1994). This flow orientation method has also been used to orient small amounts of NTs (0.1% wt) in a urethane acrylate polymer to thicknesses up to 150  $\mu\text{m}$  (Zhao and Weng 1996; Wood, Zhao et al. 2001). An alternative method that may be more suitable for larger samples is tensile loading of the NRP at temperatures above the glass transition temperature of the polymer (Jin, Bower et al. 1998; Bower, Rosen et al. 1999). A combination of solvent casting and melt mixing was also found to produce a high degree of nanotube alignment (Haggenmueller, Gommans et al. 2000). While individual SWNTs and SWNT ropes have been aligned in the presence of electric (Chen, Saito et al. 2001) and magnetic (Smith, Benes et al. 2000) fields, to our knowledge this method has yet to be extended to nanotube-reinforced polymers.

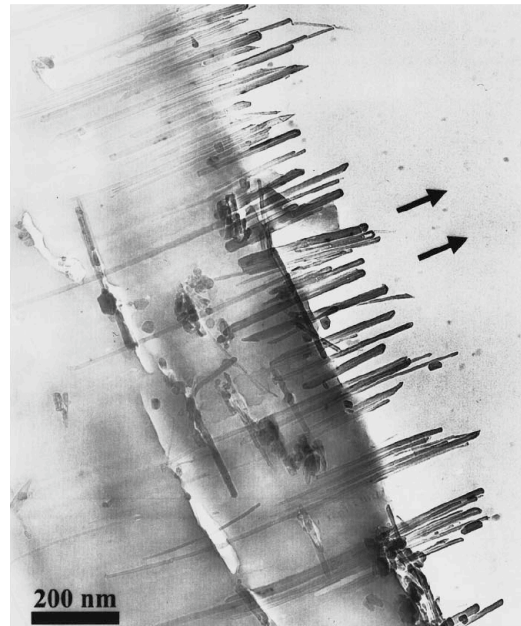


**Figure 9. Alignment of nanotubes in PHAE via microtoming . The sample thickness is 90 nm. (Jin, Bower et al. 1998)**

### **Load transfer across the nanotube-polymer interface**

Another topic of critical importance is the NT-polymer interface and load transfer between the polymer and the nanotubes (Schadler, Giannaris et al. 1998; Bower, Rosen et al. 1999; Jia, Wang et al. 1999; Shaffer and Windle 1999; Ajayan, Schadler et al. 2000; Lordi and Yao 2000; Qian, Dickey et al. 2000; Lozano and Barrera 2001). Poor load transfer for MWNTs and SWNT ropes embedded in a polymer has been attributed to the relative slipping of individual tubes within the MWNT (Schadler, Giannaris et al. 1998) and the rope (Ajayan, Schadler et al. 2000), respectively. However, other researchers have found evidence of promising nanotube-

polymer interactions in composite materials. For example, a strong interface between MWNTs and polystyrene (PS) (Qian, Dickey et al. 2000) and polyhydroxyaminoether (PHAE) (Jin, Bower et al. 1998) has been reported. Analysis of SWNT bundles-PMMA thin films found that PMMA was able to intercalate within the bundles, which would likely enhance the interface between the nanotube and polymer phases (Stéphan, Nguyen et al. 2000). Significant wetting and interfacial adhesion for SWNT bundles embedded in an epoxy resin has also been reported (Lourie and Wagner 1998b). Functionalization of the NTs to increase their chemical reactivity has also been proposed as means to further promote nanotube-polymer interaction (Srivastava, Brenner et al. 1999).

A recent molecular dynamics study suggests that polymer morphology, and specifically the helical wrapping of the polymer around the nanotubes, is a key factor influencing the strength of the interface (Lordi and Yao 2000). Using molecular mechanics to study the interfacial characteristics of a polystyrene-nanotube composite, the interfacial shear stress was estimated to be 160 MPa (Liao and Li 2001). This is comparable to the value of 500 MPa obtained from fragmentation experiments on a polyurethane-NT system, which is an order of magnitude larger than typically measured in conventional fiber-based composites (Wagner, Lourie et al. 1998). Finally, due to their demonstrated adhesion within a urethane matrix, researchers are currently interested in using NTs as nanoscale strain sensing devices. Here low

fractions of nanotubes (0.1% wt) make the host polymer Raman-active, allowing changes in the Raman spectrum to be related to strain within the material (Wood, Zhao et al. 2001; Zhao, Wood et al. 2001). While promising, a much better understanding of the factors that influence the nanotube-polymer interface is required.

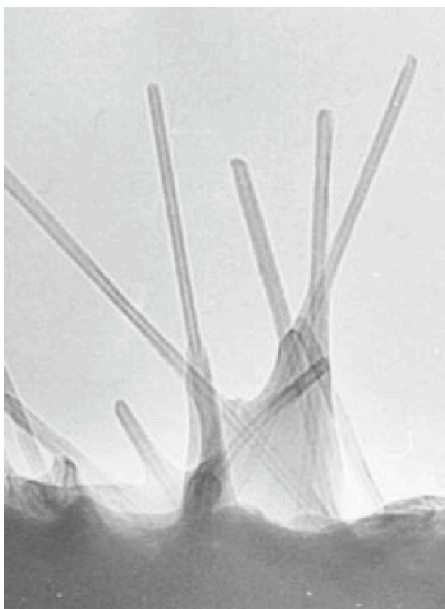


**Figure 10. TEM image showing evidence of PPV wetting the nanotubes. (Curran, Ajayan et al. 1998)**

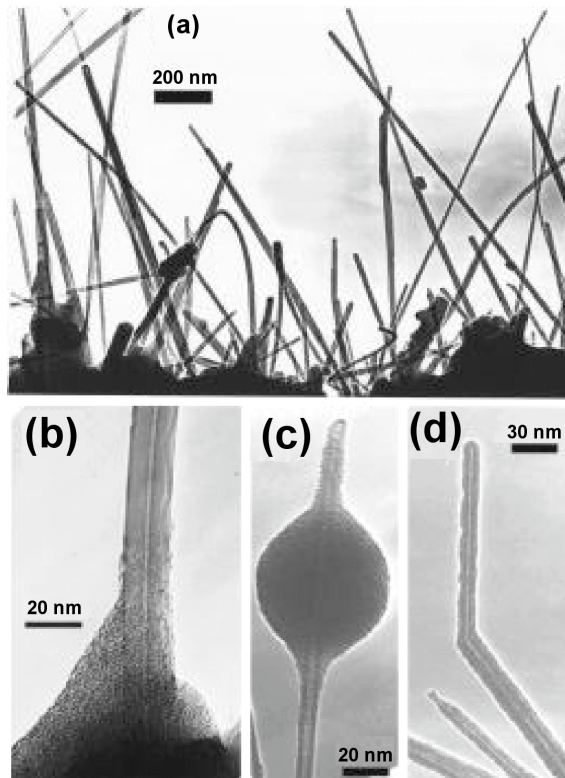


**Figure 11. TEM images of MWNTs in PHAE. (a) Fracture surface. (b,c) Evidence of good adherence between the polymer and the MWNT. (d) Plastically deformed MWNT at fracture surface. (Bower, Rosen et al. 1999)**

The three issues identified above will influence our ability to design and model materials that fully exploit the potential of nanoscale reinforcement. One issue which has not typically been associated with the modeling of NRPs, but which seems critical based on micrograph images of these materials, is the characteristic waviness or curvature of embedded nanotubes. To address how this embedded waviness influences the effective properties of these materials, we have developed a hybrid finite element-micromechanics model that integrates NT waviness into micromechanical predictions

of the NRP effective modulus. Presented in Chapter 3, this model suggests that moderate waviness, while potentially beneficial for other applications (i.e. strength), can drastically reduce the effective stiffness of the NRP when compared to straight nanotube inclusions.

### ***Mechanical Properties of Carbon Nanotube-Reinforced Polymers***

Recently a great deal of experimental work has been presented in the literature looking at the effective properties of polymers reinforced with carbon nanotubes. It is difficult to generalize across these studies because of the large number of parameters that can influence the effective properties, including the method of NT fabrication, size and form of the NT, NRP processing conditions, NT-polymer interaction, and the specifics of the polymer chemistry. However, one constant throughout much of the experimental work is that significant improvements in the properties of the NRP, with respect to that of the un-reinforced polymer, are obtained. In the following sections we highlight some of the relevant work in the literature. A more extensive listing of related work is summarized in the Appendix.

#### **Elastic behavior**

Initial experimental work looking at the effective elastic properties of carbon nanotube-reinforced polymers has suggested that significant property enhancement

can be achieved with the addition of relatively small amounts of carbon nanotubes. In perhaps the first published work in this area, 5 wt% MWNTs were mixed in an epoxy and formed into macroscale (millimeter) samples; the tensile and compression moduli measured in these experiments are given in Table 4 (Schadler, Giannaris et al. 1998).<sup>2</sup> Simultaneous Raman spectroscopy measurements were used to qualitatively measure the strain in the nanotubes as the samples were loaded, and it was reported that the Raman peak position only shifted significantly in compression. It has been suggested that this is evidence that only the outer layer of the MWNT was loaded in tension, whereas all layers of the MWNT are loaded in compression. While poor load transfer between adjacent shells in a MWNT is likely, as they only interact via van der Waals interactions, it is worth noting the both the average tensile and compression moduli in this study increased by approximately 20% in comparison to the response of the pure polymer.

Work with PMMA-based NRPs found that pre-processing CVD-grown MWNTs using a ball mill (treated NTs) resulted in an increase in tensile strength as shown in Table 5 (Jia, Wang et al. 1999). The strength enhancement seen with the NT treatment was attributed to the ball milling operation separating the individual nanotubes (in comparison to the entangled untreated NTs). They also reported that

---

<sup>2</sup> The authors of this study also noted that SEM images show the embedded NTs remain “curved and interwoven” in the NRP, an observation that led to the model described in Chapter 3 incorporating nanotubes waviness into effective moduli predictions for an NRP.

increasing the PMMA polymerization time, prior to adding the NTs, allowed the PMMA molecules to grow larger and wrap the NT. Finally, the authors suggest that the initiator used in the polymerization process (AIBN) may interact with the nanotubes, opening  $\pi$ -bonds that are then free to form bonds with the polymer. SEM images of the fracture surfaces show that the nanotubes are wrapped with PMMA layers, which they suggest is an indication of a strong interface between the phases.

| Material   | Tensile Modulus (GPa) | Compression modulus (GPa) |
|------------|-----------------------|---------------------------|
| Pure epoxy | $3.1 \pm 0.2$         | $3.63 \pm 0.25$           |
| NRP        | $3.71 \pm 0.5$        | $4.5 \pm 1.5$             |

**Table 4. Tensile and compressive moduli for 5% MWNTs in epoxy (Schadler, Giannaris et al. 1998).**

| NT wt% | Tensile strength (MPa) |             |
|--------|------------------------|-------------|
|        | Untreated NTs          | Treated NTs |
| 0      | 54.90                  | 54.90       |
| 1      | ~21                    | 58.70       |
| 3      | ~20                    | 66.80       |
| 5      | NA                     | 71.66       |
| 7      | NA                     | 71.65       |
| 10     | NA                     | 47.15       |

**Table 5. Tensile strength for PMMA-based NRP with treated and untreated MWNTs. (Jia, Wang et al. 1999)**

Researchers at the University of Kentucky have published experimental work measuring the tensile moduli and strength of 1 wt% MWNTs in polystyrene. A homogeneous distribution (on the  $\mu\text{m}$  scale) of MWNTs was achieved by an ultrasound-assisted solution-evaporation method. They found a 25% increase in the tensile strength and an approximately 40% increase in the tensile modulus, with both values being relatively independent of nanotube length. TEM images suggest that cracks propagate in regions of relatively low NT density, and that the MWNTs tend to align and bridge the crack prior to failure (see Figure 12). Eventual failure of the NRP was due to either NT fracture or pull-out from the matrix. Because NTs aligned parallel to the direction of crack propagation tended to break between the crack faces

(rather than pull-out from the matrix), the authors concluded that a relatively strong interface exists between the two phases.

More recent work from the same Kentucky group has looked at the effective NRP modulus for variable loadings of MWNTs in polystyrene (Andrews, Jacques et al. 2002). The CVD grown MWNTs have an average diameter of about 25 nm and are approximately 40  $\mu\text{m}$  long prior to NRP processing. As a means to develop a processing method that would be compatible with industry capabilities, the samples were prepared by shear mixing in a Haake PolyLab bowl mixer using roller rotors. Such a procedure has been reported to yield excellent dispersion (Andrews 2001). One drawback of this fabrication method is that it may shorten the length of the nanotubes. Those researchers, however, believe that mild enough conditions were used such that this shortening was negligible.

The tensile moduli values obtained in this study are shown in Figure 13 and compared with the standard Rule of Mixtures upper and lower bounds and a micromechanics (Mori-Tanaka) model assuming a 3D random orientation of nanotubes with a nanotube modulus of 450 GPa (Fisher, Bradshaw et al. 2002b).<sup>3</sup> Within the NRP the nanotubes are likely to randomly orientated in three-dimensional space, which reduces the optimal effective modulus by approximately a factor of four

---

<sup>3</sup> The nanotube modulus of 450 GPa used here is an estimate based on experimental measurements made on similarly grown CVD MWNTs (Pan, Xie et al. 1999; Andrews 2001).

(when compared to the case of aligned nanotubes, which is closely modeled by the Rule of Mixtures upper bound). The experimental modulus enhancements shown here are not as substantial as reported in other works, which is attributed to insufficient bonding between the nanotubes and the matrix as verified in TEM images showing significant nanotube pullout from the polymer (Andrews 2001). Improvements in the interfacial characteristics of this particular system may result in even larger improvements in effective properties.

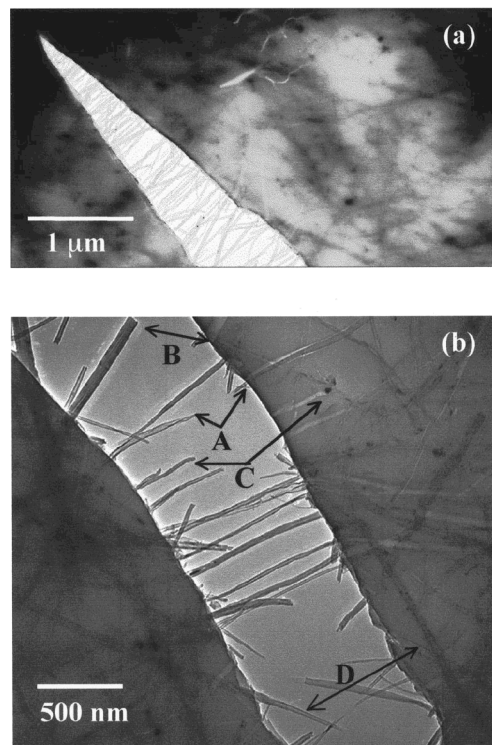


**Figure 12. TEM observation of crack propagation and nanotube crack bridging in an epoxy-MWNT sample. (Qian, Dickey et al. 2000)**

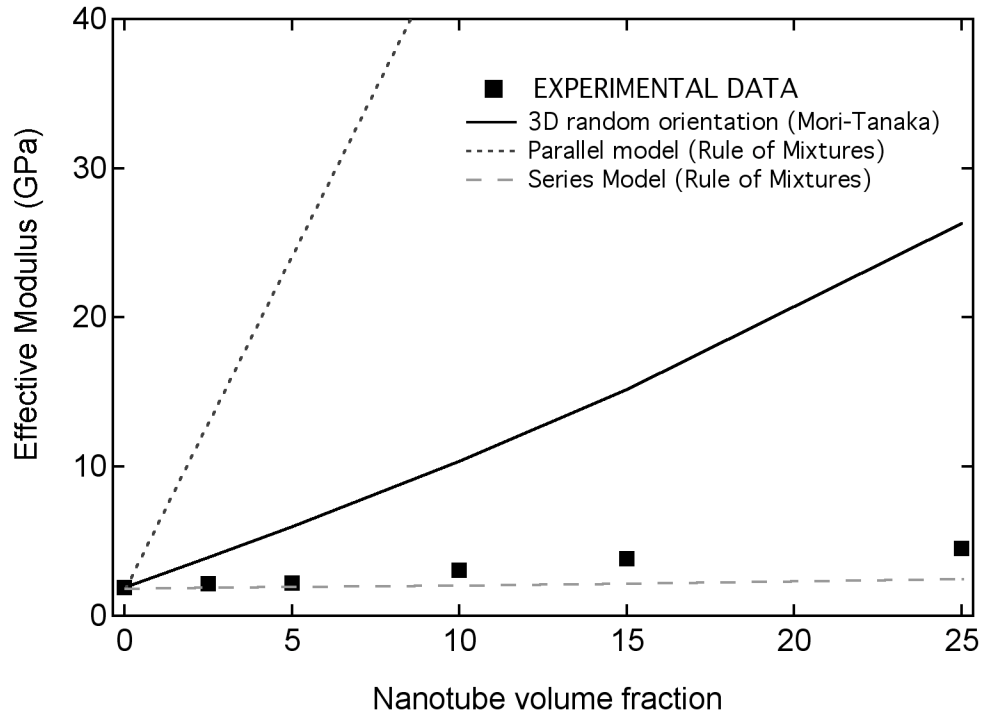


**Figure 13. Comparison of experimental data for MWNTs in polystyrene (Andrews, Jacques et al. 2002) with Rule of Mixtures and Mori-Tanaka predictions.**

### Viscoelastic behavior

In addition to the work discussed above, a limited amount of experimental research has looked at the effective viscoelastic (time- and temperature-dependent) behavior of nanotube-reinforced polymers. Because the nanotubes are on the same size scale as the polymer chains, they are expected to alter the mobility of the polymer chains and thus change the viscoelastic response of the NRP with respect to the un-

reinforced polymer. Probing the mechanical response of the NRP as a function of temperature typically shows four characteristic changes in the material response as shown Figure 14 and Figure 15:

1. Increases in the low temperature (below the polymer glass transition temperature  $T_g$ ) storage modulus, similar to the elastic behavior discussed previously,
2. Significant increases in the high temperature (above  $T_g$ ) response of the material,
3. Shifting of the effective glass transition temperature of the material, usually to temperatures greater than the  $T_g$  of the polymer,
4. Broadening of the loss moduli and loss tangent peaks, suggesting the presence of polymer regions exhibiting non-bulk polymer properties.

Examples of the temperature-dependent response of nanotube-reinforced polymers are shown in Figure 14 and Figure 15 for MWNTs in epoxy (with and without surfactant) and PVOH, respectively. In Figure 14, comparing the response of the pure epoxy (curve 1) to that of the epoxy-1% MWNTs-surfactant sample (curve 4) shows a 25 °C shift in the glass transition temperature (from 63 to 88 °C), as measured by the peak of the loss tangent curve. A smaller shift in  $T_g$  was also seen when the NRP was processed without surfactant (see curve 3). Storage moduli results for these

samples show increases of over 30% for the NRP processed with surfactant. The greater property improvements observed with the use of surfactant were attributed to better nanotube dispersion within these samples.

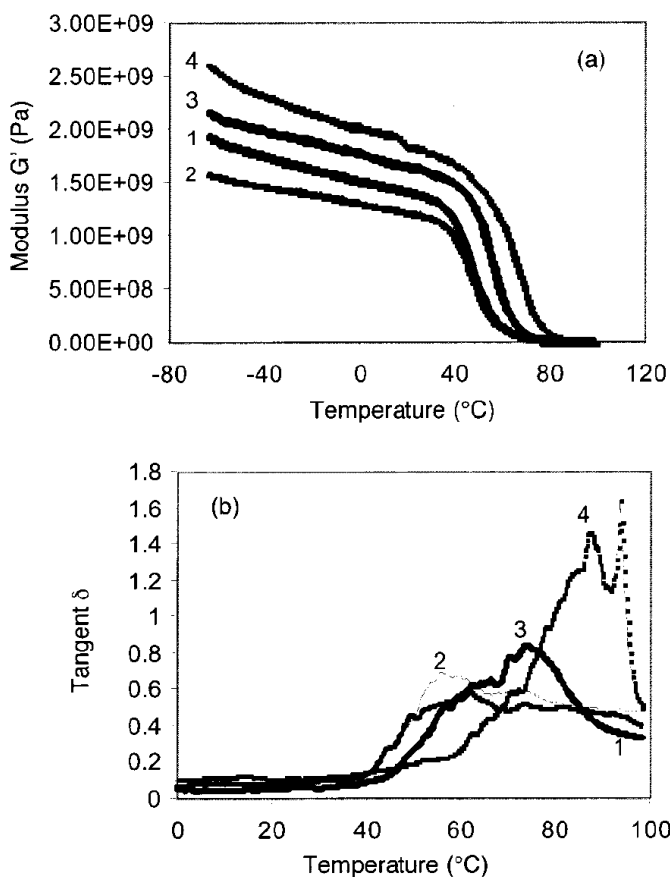


**Figure 14. Storage modulus and loss tangent results via dynamic mechanical analysis for different epoxy samples. Curves are labeled as: (1) pure epoxy, (2) epoxy plus  $\text{C}_{12}\text{EO}_8$  surfactant, (3) epoxy plus 1% wt MWNTs, and (4) epoxy plus surfactant plus 1% wt MWNTs. (Gong, Liu et al. 2000).**

Similar changes in viscoelastic behavior have been seen with MWNTs incorporated into poly(vinyl alcohol) (PVOH) as shown in Figure 15. Composite films were made by a solution casting process, followed by controlled evaporation to produce thin films with thicknesses on the order of 50  $\mu\text{m}$ .<sup>4</sup> While the peak of the loss tangent curve does not appear to shift with the addition of the nanotubes (for all samples the  $T_g$  was found to be between 75 and 80  $^\circ\text{C}$ ), the high-temperature portion of the peak broadens as the fraction of nanotubes increases. This was attributed to a reduction of polymer chain mobility in the reinforced samples. Polymers reinforced with vapor-grown carbon nanofibers (diameters of 20-200 nm) (Lozano and Barrera 2001), nano-sized cellulose whiskers (Brechet, Cavaille et al. 2001), and various nanoclays (Liu and Wu 2002; Wu, Liu et al. 2002; Xiao, Sun et al. 2002) have also been found to have a viscoelastic response significantly different than that of the bulk polymer.

Based on these findings, we have conducted dynamic mechanical testing of MWNTs embedded in polycarbonate to study different viscoelastic characteristics (glass transition temperature, relaxation spectra, and physical aging) of the material. Our results for each mode of viscoelastic response are consistent with the hypothesis

---

<sup>4</sup> Based on other work in the literature it seems surprising that NRP samples with up to 60 wt% MWNTs have been successfully fabricated. While the property enhancements with larger amounts of nanotubes are still significant, it is likely that the dispersion of the nanotubes within these samples was quite poor.

that within the NRP there are regions of polymer in the vicinity of the nanotubes with reduced mobility; we model this as an interphase region with viscoelastic properties different from that of the bulk polymer. This work is discussed in much greater detail in Chapter 4 of this dissertation.

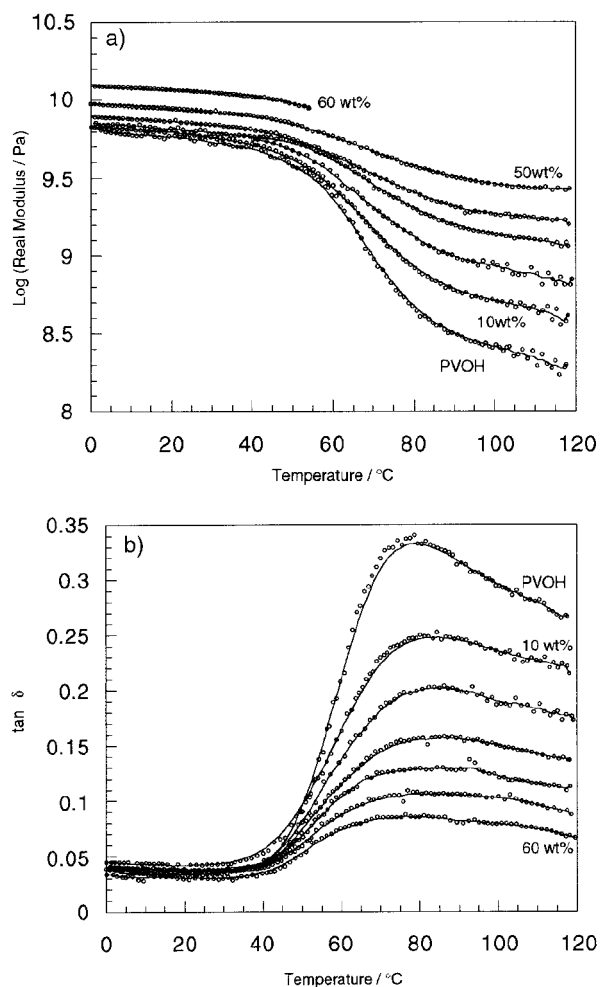


**Figure 15. Dynamical mechanical analysis of PVOH with different loadings of CVD grown nanotubes. (Shaffer and Windle 1999)**

## Other properties

While the work in this dissertation focuses on the mechanical behavior of NRPs, other researchers are looking to leverage the extraordinary electrical and thermal conductivities of the nanotubes to create multifunctional materials with improved electrical and thermal properties. For example, the addition of low volume fractions of NTs is being pursued as a means to increase the conductivity of insulating polymers from  $\sim 10^{-9}$  S/m to  $10^{-6}$  S/m, the level required to provide electrostatic discharge and electromagnetic-radio frequency interference protection (Sandler, Shaffer et al. 1999; Shaffer and Windle 1999). Often in such cases, any improvements in mechanical properties are viewed as an additional benefit; what is more critical is that the optical properties and finish of the sample remain unchanged.

The impact of the nanotubes on the effective electrical conductivity of NRPs are shown in Figure 16 and Figure 17 for CVD nanotubes in epoxy and arc grown MWNTs in poly(*m*-phenylenevinylene-*co*-2,5-dioctoxy-*p*-phenyleneviylene) (PmPV), respectively. In each case substantial increases in conductivity have been attributed to a percolation-type process, which is achievable for relatively low volume (weight) fractions of the nanotubes due to their high aspect ratio and outstanding conducting properties. As shown in Figure 16, the nanotubes are much more efficient than the carbon black filler which is currently added to improve polymer conductivity. Similar

increases in thermal conductivity using small amounts of nanotubes have also been reported (Biercuk, Llaguno et al. 2002).

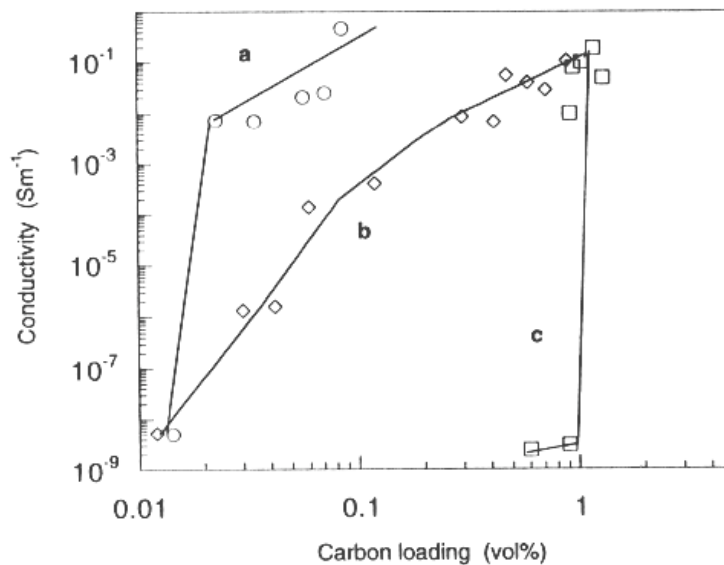


**Figure 16. Electrical conductivity of CVD grown NTs in an epoxy. (a) CVD grown NTs. (b) carbon black with copper-chloride. (c) carbon black only. (Sandler, Shaffer et al. 1999)**

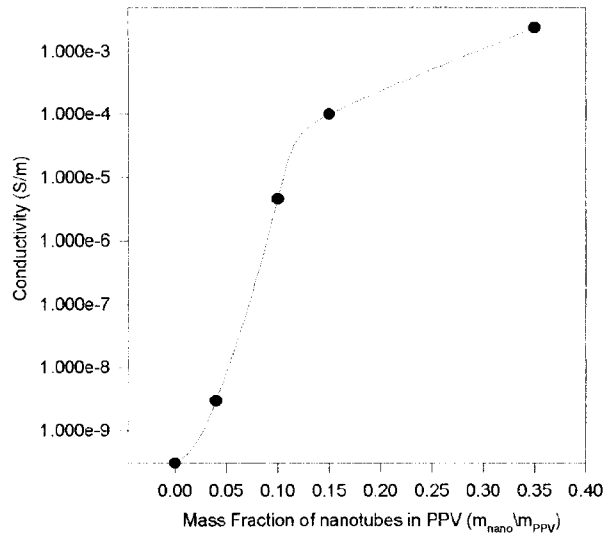


**Figure 17. Electrical conductivity of PmPV/nanotube composites. (Curran, Ajayan et al. 1998)**

For purposes of this dissertation we will limit our discussion to the mechanical behavior of polymers reinforced with small volume fractions of carbon nanotubes. Our focus is on the extension of traditional micromechanics and viscoelastic models for the study of nanotube-reinforced polymers, so that from these models we can start to better understand the impact of the nanotubes on the mechanical response of the material. Two models have been developed in this regard, and will be presented in the next two chapters:

- In Chapter 3, we present a hybrid finite element – micromechanics model that incorporates the typically observed waviness of embedded nanotubes into micromechanics predictions of the effective elastic modulus of an NRP.

- In Chapter 4, we present experimental evidence of a reduced mobility, non-bulk polymer region, which we attribute to the interaction between the nanotubes and the polymer chains. The effect of this interaction is modeled as a shift in the relaxation times of the non-bulk polymer properties and results in a change in the effective viscoelastic properties of the NRP.

The results presented in this chapter demonstrate the complexity of modeling the effective behavior of NRPs. The models presented in the next chapters represent initial efforts to extend existing constitutive models in order to meet this challenge.